

The simplest model to explain the vibrational level structure of protonated methane?

Jonathan I. Rawlinson*

School of Mathematics, University of Bristol, Bristol, UK

Csaba Fábri and Attila G. Császár

Laboratory of Molecular Structure and Dynamics,

Institute of Chemistry, Eötvös Loránd University,

Pázmány Péter sétány 1/A, H-1117 Budapest, Hungary and

MTA-ELTE Complex Chemical Systems Research Group, P.O. Box 32, H-1518 Budapest 112, Hungary

(Dated: February 28, 2025)

A new one-dimensional model is proposed for the low-energy vibrational quantum dynamics of CH_5^+ based on the motion of an effective particle confined to a 4-regular (quartic) 60-vertex metric graph Γ_{60} with a single edge length parameter. Within this model, the quantum states of CH_5^+ are obtained in analytic form and are related to combinatorial properties of Γ_{60} . In particular, we show that the bipartite structure of Γ_{60} gives a simple explanation for curious symmetries observed in numerically exact variational calculations on CH_5^+ .

Protonated methane, CH_5^+ , also called methonium, is considered to be the prototype of pentacoordinated non-classical carbonium ions [1–3]. The curious carbonium cations yielded an extremely rich chemistry and a Nobel-prize to their discoverer, George Olah [4]. Nevertheless, these are not the only sources of fame for carbonium ions and in particular for CH_5^+ . Over the last two decades [5], CH_5^+ has been posing a formidable challenge to high-resolution spectroscopists [5–15]. The most outstanding issue is that the spectrum of CH_5^+ is exceptionally complex even at extremely low temperatures [9, 13] due to its quasistructural nature [16].

On the computational side, accurate rovibrational energy levels and eigenstates have been made available for CH_5^+ , owing to huge numerical efforts, in recent years [7, 12, 14]. These studies have revealed close-lying clusters in the rovibrational energy levels, with fascinating symmetries. These features have defied explanation by conventional means, motivating the development of novel models for CH_5^+ . The most important models put forward so far are as follows: (a) particle-on-a-sphere (POS) [17–23], (b) five-dimensional (5D) rotor (superrotor) [24–26] and (c) quantum graph [15, 27]. So far, the quantum-graph model seems to result in the most satisfactory explanation of the low-energy quantum dynamics of CH_5^+ , including both vibrations [15] and rotations [27].

Quantum graphs have a long history, dating back to Linus Pauling’s description of electrons in organic molecules in the 1930s [28]. They have only recently been introduced to the study of nuclear dynamics, where they have proved useful in high-resolution spectroscopy [15, 27] and also α -cluster dynamics in nuclear physics [29, 30]. Quantum graphs [31] are metric graphs, that is each of their edges possesses a length. In the context of rovibrational dynamics of molecules, each vertex of the graph represents a version [32] of an equilibrium structure. The vertices are connected by edges which represent collective internal motions converting different

versions into each other. Once a quantum graph is set up, one constructs the one-dimensional Schrödinger equation for a particle confined to the graph and solves it to determine the energy levels and eigenstates (see the Supplemental Material). In this way, complex multidimensional quantum dynamics is mapped onto the effective motion of a one-dimensional particle confined to a much simpler space.

In the case of CH_5^+ , the equilibrium structure is composed of a H_2 unit sitting on top of a CH_3^+ tripod, an arrangement with C_s point-group symmetry. The five protons can be rearranged in $5!=120$ ways, generating 120 symmetry-equivalent versions, which become the 120 vertices of a quantum graph Γ_{120} [15], illustrated in Fig. 1. There are two types of motion interconverting the 120

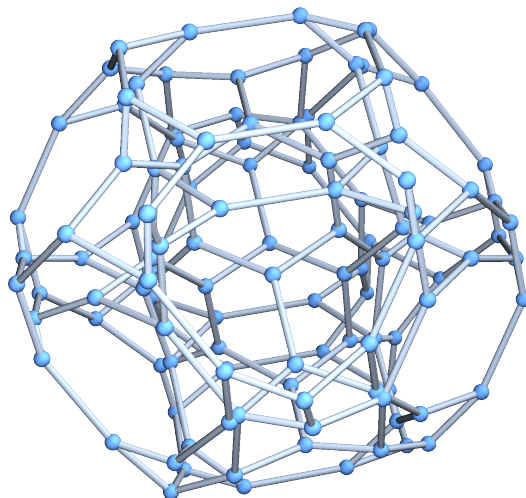


FIG. 1. Illustration of the 3-regular quantum graph Γ_{120} . In this model of the quantum dynamics of CH_5^+ there are two distinct edge lengths, corresponding to internal rotations of the H_2 unit by 60° and the flip motion that exchanges a pair of protons between the H_2 and CH_3^+ units.

TABLE I. The block structure characterizing the first 60 vibrational states of CH_5^+ , revealed in variational computations [12, 14]. The numbers in parentheses give the total number of positive and negative parity states within a block, reflecting the degeneracy of the states.

Block 1	Block 2
$0 - 60 \text{ cm}^{-1} (15,15)$	$110 - 200 \text{ cm}^{-1} (15,15)$
$A_1^+ \oplus G_1^+ \oplus H_1^+ \oplus H_2^+ \oplus$ $G_2^- \oplus H_2^- \oplus I^-$	$G_1^+ \oplus H_1^+ \oplus I^+ \oplus$ $A_2^- \oplus G_2^- \oplus H_1^- \oplus H_2^-$

equivalent versions: the internal rotations of the H_2 unit by 60° (both clockwise and counterclockwise), and the flip motion that exchanges a pair of protons between the H_2 and CH_3^+ units (see Fig. 2 for the local structure of Γ_{120}). Given our knowledge about the stationary points of the potential energy hypersurface of CH_5^+ [33], it is plausible that motions other than the internal rotation and flip motions can be disregarded as long as one is interested in the low-energy rovibrational quantum dynamics of CH_5^+ , and so one takes these motions to correspond to the edges of Γ_{120} . As one flip edge and two internal rotation edges are connected to each vertex of Γ_{120} , each vertex has a degree of three (Γ_{120} is a 3-regular graph). The 120 internal rotation and 60 flip edges are assigned effective lengths L_{rot} and L_{flip} , respectively.

The quantum graph Γ_{120} reproduces the low-energy rovibrational energy levels of CH_5^+ , as well as of CD_5^+ , remarkably well when optimized values of L_{flip} and L_{rot} are used [15, 27] (see the Supplemental Material for the numerical values of the edge length parameters and the vibrational energy levels of CH_5^+). For instance, the Γ_{120} model perfectly reproduces the block structure (states occurring in groups of 30) of the vibrational eigenstates of CH_5^+ , first noted in a variational study of Wang and Carrington [12] and later confirmed in [14] (see Table I). Rovibrational eigenstates of CH_5^+ are labelled by irreducible representations (irreps) of the molecular symmetry (MS) group $S_5^* = S_5 \times \{E, E^*\}$, generated by S_5 permutations of the five protons together with spatial inversion E^* (E denotes the identity operation).

Beyond the existence of blocks, we have noticed other clear symmetry relations for the first 60 quantum states. A comparison of the group-theoretic relation

$$(A_1^+ \oplus G_1^+ \oplus H_1^+ \oplus H_2^+) \otimes A_2^- \simeq A_2^- \oplus G_2^- \oplus H_2^- \oplus H_1^- \quad (1)$$

with the data in Table I suggests a direct correspondence between the 15 positive-parity states in Block 1 [appearing on the left-hand side (LHS) of Eq. (1)] and the 15 negative-parity states in Block 2 [right-hand side (RHS) of Eq. (1)]. Likewise,

$$(G_2^- \oplus H_2^- \oplus I^-) \otimes A_2^- \simeq G_1^+ \oplus H_1^+ \oplus I^+, \quad (2)$$

suggesting a link between the 15 negative-parity states in

Block 1 and the positive-parity states in Block 2. These remarkable relations have been lacking any simple explanation, even in terms of the Γ_{120} model. One purpose of this Letter is to introduce an even simpler quantum graph model, derived from Γ_{120} , which explains these symmetries.

Let us start with the Γ_{120} model. Following our original study [15], we neglect the potential energy along the edges of Γ_{120} , since the barriers to the internal rotation and flip motions are small (about 30 cm^{-1} and 300 cm^{-1} , respectively). The edge lengths L_{flip} and L_{rot} were fixed in Ref. [15] by an optimization procedure. The flip edges were assigned a much smaller effective length than the internal rotation edges, with the optimized values satisfying $L_{\text{flip}}/L_{\text{rot}} \approx 1/60$.

Our new model is based on the following idea: the ratio $L_{\text{flip}}/L_{\text{rot}}$ is so small that it is tempting to imagine shrinking the flip edges to zero length, effectively identifying the two vertices at the endpoints of each flip edge to give a single vertex. In this way the number of vertices is halved and we get a new graph Γ_{60} with only the internal rotation edges remaining. It seems reasonable to identify each new vertex with the midpoint of the (now contracted) flip edge, which is a C_{2v} -symmetric transition state, as illustrated in Fig. 2. There are 60 symmetry-equivalent versions of this configuration, and we propose that the low-energy quantum states can be understood in terms of motion between these versions. Each vertex is connected to precisely four other vertices, as shown also in Fig. 2, giving rise to the 4-regular (quartic) quantum

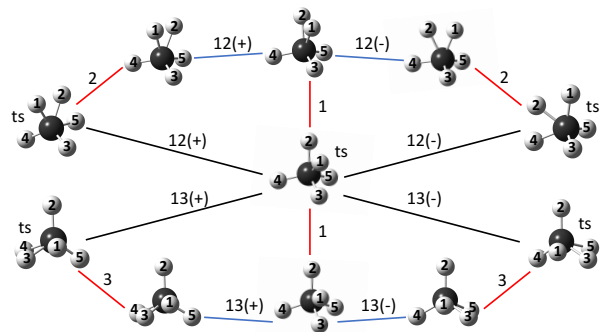


FIG. 2. Local structure of the quantum graphs Γ_{120} (blue and red edges) and Γ_{60} (black edges). The red edges correspond to the flip motion and the labels indicate which proton is exchanged from a H_2 unit to a CH_3^+ unit. The blue edges correspond to an internal rotation and the labels indicate the H_2 unit which rotates relative to the CH_3^+ unit in a clockwise (+) or anticlockwise (-) fashion. The midpoint of each red flip edge is a C_{2v} -symmetric transition state (ts). In going from Γ_{120} to Γ_{60} , the red edges shrink so that we are left with just the transition states connected by black edges.

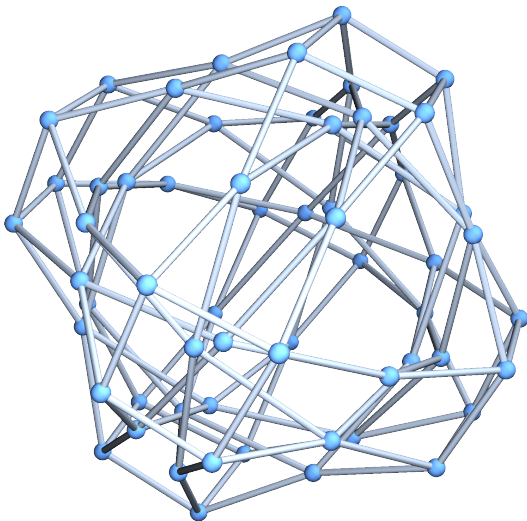


FIG. 3. Illustration of the 4-regular quantum graph Γ_{60} . In this model of the quantum dynamics of CH_5^+ there is a single edge length, connecting versions of C_{2v} -symmetric transition states, midpoints of the flip edge of Γ_{120} .

graph Γ_{60} , which is illustrated in Fig. 3.

An alternative way of rationalizing this contraction procedure is as follows: at the energies we are interested in, one can show that the Γ_{120} wave functions for the energy eigenstates are approximately constant along the flip edges. In this limit, the boundary conditions of Γ_{120} become equivalent to those of Γ_{60} (see the Supplemental Material for an explanation).

We now seek the quantum states corresponding to motion on the Γ_{60} graph. The eigenenergies are found by solving the time-independent Schrödinger equation for a free particle moving along the edges, with the so-called Neumann boundary conditions [31] imposed on the eigenstates. These conditions are that the wave function should be continuous everywhere, with zero total momentum flux out of each vertex. As we have already pointed out, Γ_{60} is a 4-regular graph with all edges having a common length $l = L_{\text{rot}}$. Perhaps surprisingly, these properties imply that the structure of the quantum energy levels can be determined entirely through consideration of *combinatorial properties* of the graph.

More precisely, given a wave function ψ defined on the graph Γ_{60} and obeying the time-independent Schrödinger equation along each edge,

$$-\frac{1}{2} \frac{d^2\psi}{dx^2} = E\psi, \quad (3)$$

consider the vector of its values at each vertex $\mathbf{v} = (\psi(v_1), \psi(v_2), \dots)$. It is straightforward to prove, see the Supplemental Material, that ψ is an eigenfunction with energy E satisfying the Neumann boundary conditions if and only if

$$\mathbf{A}\mathbf{v} = 4 \cos(\sqrt{2El}) \mathbf{v}, \quad (4)$$

i.e., if and only if $\lambda = 4 \cos(\sqrt{2El})$ is an eigenvalue of the *adjacency matrix* \mathbf{A} for the graph Γ_{60} , with \mathbf{v} in the corresponding eigenspace. \mathbf{A} is simply a matrix whose elements indicate whether given pairs of vertices are connected by an edge or not, and is a familiar concept in elementary graph theory [34]. Its entries are given by

$$(A)_{ij} = \begin{cases} 1 & \text{if vertices } v_i, v_j \text{ connected} \\ 0 & \text{otherwise} \end{cases}. \quad (5)$$

The factor of 4 on the RHS of Eq. (4) corresponds to the fact that each vertex connects to precisely 4 other vertices.

Equation (4) therefore relates the *quantum spectrum* (the eigenvalues of the Hamiltonian) to the so-called *combinatorial spectrum* (the eigenvalues of the adjacency matrix). The combinatorial spectrum is a concept already utilized in molecular spectroscopy [35], and only depends on the connectivity of the graph as encoded in \mathbf{A} .

To find the combinatorial spectrum of Γ_{60} , we look for roots of the characteristic polynomial $\chi_{\mathbf{A}}(\lambda) = \det(\lambda\mathbf{I} - \mathbf{A})$ associated with the adjacency matrix \mathbf{A} . An explicit expression for \mathbf{A} is easily derived by considering paths of the form illustrated in Fig. 2. In the end, we obtain

$$\chi_{\mathbf{A}}(\lambda) = (\lambda^4 - 9\lambda^2 + 16)^5 (\lambda^4 - 12\lambda^2 + 16)^4 (\lambda^2 - 1)^{11} (\lambda^2 - 16), \quad (6)$$

and the full combinatorial spectrum is given in Table II. Table II also shows the dimensions of the corresponding eigenspaces and the irreps corresponding to the symmetry action of the MS group S_5^* by graph automorphisms.

We pause here to note the striking similarity between the symmetry information of Tables I and II. First, note

TABLE II. The combinatorial spectrum of the quantum graph Γ_{60} , where $\dim(\lambda)$ gives the degeneracy of a given eigenvector corresponding to the eigenvalue λ [see Eq. (6)].

λ	$\dim(\lambda)$	S_5^* irrep
4	1	A_1^+
$1 + \sqrt{5}$	4	G_2^-
$\frac{1}{2}(1 + \sqrt{17})$	5	H_1^+
$\frac{1}{2}(-1 + \sqrt{17})$	5	H_2^-
$-1 + \sqrt{5}$	4	G_1^+
1	11	$H_2^+ \oplus I^-$
-1	11	$H_1^- \oplus I^+$
$1 - \sqrt{5}$	4	G_2^-
$\frac{1}{2}(1 - \sqrt{17})$	5	H_1^+
$\frac{1}{2}(-1 - \sqrt{17})$	5	H_2^-
$-1 - \sqrt{5}$	4	G_1^+
-4	1	A_2^-

that the combinatorial spectrum splits into positive λ and negative λ , with each corresponding to a total eigenspace dimension of 30. Moreover, the eigenspaces associated with positive λ transform in precisely the same irreps as Block 1 of Table I, while those associated with negative λ transform precisely like Block 2. Thus, purely combinatorial properties of the quantum graph Γ_{60} have captured the block structure of the lowest vibrational states of CH_5^+ . Even more interestingly, we seem to have an explanation for the curious relationship between Block 1 states and Block 2 states: this corresponds to $\lambda \rightarrow -\lambda$ (see the Supplemental Material). The symmetry of the spectrum of Γ_{60} under $\lambda \rightarrow -\lambda$ is actually a simple consequence [34] of the fact that the quantum graph Γ_{60} is *bipartite*: the set of vertices V can be divided into two disjoint and independent sets A and B such that every edge connects a vertex in A to one in B . The set A is mapped to the set B by any odd permutation of the protons.

Equation (4) relates the combinatorial spectrum to the quantum spectrum, which is nicely illustrated in Fig. 4. In particular, we can see the consequences of the $\lambda \rightarrow -\lambda$ symmetry for the quantum energy levels: each state in Block 1 comes with a partner in Block 2, with their corresponding values of $\sqrt{2El}$ being related by reflection in the line $\sqrt{2El} = \pi/2$. In particular, the sum of the square roots of their energies is independent of which pair we pick, implying that the dimensionless ratios

$$\frac{\sqrt{E_1(I^-)} + \sqrt{E_2(I^+)}}{\sqrt{E_1(H_1^+) + \sqrt{E_2(H_2^-)}}, \frac{\sqrt{E_1(H_2^+) + \sqrt{E_2(H_1^-)}}}{\sqrt{E_1(H_1^+) + \sqrt{E_2(H_2^-)}}, \dots \quad (7)$$

are all equal to 1 in the Γ_{60} model. This compares very favourably with the variational seven-dimensional model

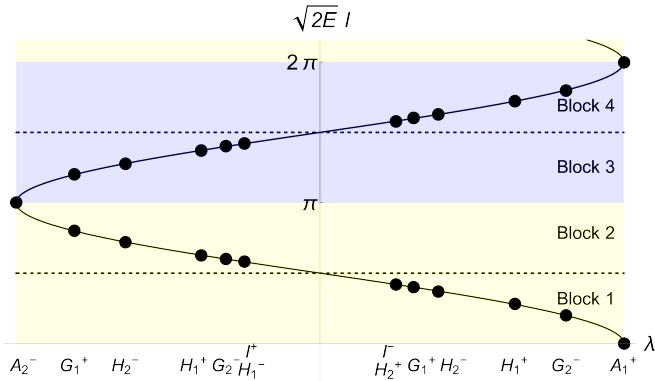


FIG. 4. Illustration of the block structure and the symmetry properties of the spectrum of the quantum graph Γ_{60} . Black dots indicate energies of the quantum states.

[7, 12, 14] results

$$\frac{\sqrt{E_1(A_1^+) + \sqrt{E_2(A_2^-)}}}{\sqrt{E_1(H_1^+) + \sqrt{E_2(H_2^-)}}} \approx \frac{\sqrt{0} + \sqrt{198}}{\sqrt{20} + \sqrt{139}} \approx 0.86, \quad (8)$$

$$\frac{\sqrt{E_1(G_2^-) + \sqrt{E_2(G_1^+)}}}{\sqrt{E_1(H_1^+) + \sqrt{E_2(H_2^-)}}} \approx \frac{\sqrt{10} + \sqrt{154}}{\sqrt{20} + \sqrt{139}} \approx 0.95, \quad (9)$$

$$\frac{\sqrt{E_1(H_2^-) + \sqrt{E_2(H_1^+)}}}{\sqrt{E_1(H_1^+) + \sqrt{E_2(H_2^-)}}} \approx \frac{\sqrt{41} + \sqrt{122}}{\sqrt{20} + \sqrt{139}} \approx 1.07, \quad (10)$$

$$\frac{\sqrt{E_1(G_1^+) + \sqrt{E_2(G_2^-)}}}{\sqrt{E_1(H_1^+) + \sqrt{E_2(H_2^-)}}} \approx \frac{\sqrt{49} + \sqrt{113}}{\sqrt{20} + \sqrt{139}} \approx 1.08, \quad (11)$$

$$\frac{\sqrt{E_1(I^-) + \sqrt{E_2(I^+)}}}{\sqrt{E_1(H_1^+) + \sqrt{E_2(H_2^-)}}} \approx \frac{\sqrt{58} + \sqrt{112}}{\sqrt{20} + \sqrt{139}} \approx 1.12, \quad (12)$$

and

$$\frac{\sqrt{E_1(H_2^+) + \sqrt{E_2(H_1^-)}}}{\sqrt{E_1(H_1^+) + \sqrt{E_2(H_2^-)}}} \approx \frac{\sqrt{59} + \sqrt{114}}{\sqrt{20} + \sqrt{139}} \approx 1.12. \quad (13)$$

In this Letter we have drastically simplified the quantum graph model of the low-energy rovibrational quantum dynamics of CH_5^+ by reducing the original 120-vertex quantum graph to a 60-vertex graph, Γ_{60} . Γ_{60} was constructed by shrinking the edges corresponding to the flip motion that exchanges a pair of protons between the H_2 and CH_3^+ units of the equilibrium structure of CH_5^+ . The quantum states of Γ_{60} are obtained in analytic form, with the structure of the energy levels depending only on combinatorial properties. The bipartite structure of Γ_{60} gives a natural explanation for symmetries in the vibrational energy levels of CH_5^+ , in good agreement with the results of numerically exact variational nuclear dynamics computations. Note that neither the variational quantum-chemical computations [7, 12, 14] nor the quantum-graph models [15, 27] yield only the Pauli-allowed states of CH_5^+ (states with A_2^\pm , G_2^\pm , and H_2^\pm symmetry have non-zero spin-statistical weights), and thus our discussion focused on *all* possible states; the non-existing states can be filtered out *a posteriori*.

The work of JIR was supported by the EPSRC grant CHAMPS EP/P021123/1. The work performed in Budapest received support from NKFIH (grant no. K119658) and from the ELTE Institutional Excellence Program (TKP2020-IKA-05) financed by the Hungarian Ministry of Human Capacities.

* Corresponding author.

jonathanianrawlinson@gmail.com.

- [1] G. A. Olah and R. H. Schlosberg, *J. Am. Chem. Soc.* **90**, 2726 (1968).
- [2] G. A. Olah, G. Klopman, and R. H. Schlosberg, *J. Am. Chem. Soc.* **91**, 3261 (1969).
- [3] G. A. Olah, *Carbocations and Electrophilic Reactions* (VCH-Wiley Publishers, Weinheim, 1974).
- [4] G. A. Olah, “My search for carbocations and their role in chemistry,” in *Les Prix Nobel en 1994* (1994) pp. 149–176.
- [5] E. T. White, J. Tang, and T. Oka, *Science* **284**, 135 (1999).
- [6] O. Asvany, P. Padma Kumar, B. Redlich, I. Hegemann, S. Schlemmer, and D. Marx, *Science* **309**, 1219 (2005).
- [7] X.-G. Wang and T. Carrington Jr., *J. Chem. Phys.* **129**, 234102 (2008).
- [8] S. D. Ivanov, O. Asvany, A. Witt, E. Hugo, G. Mathias, B. Redlich, D. Marx, and S. Schlemmer, *Nat. Chem.* **2**, 298 (2010).
- [9] O. Asvany, K. M. T. Yamada, S. Brünken, A. Potapov, and S. Schlemmer, *Science* **347**, 1346 (2015).
- [10] R. Wodraszka and U. Manthe, *J. Phys. Chem. Lett.* **6**, 4229 (2015).
- [11] H. Schmiedt, S. Schlemmer, and P. Jensen, *J. Chem. Phys.* **143**, 154302 (2015).
- [12] X.-G. Wang and T. Carrington, *J. Chem. Phys.* **144**, 204304 (2016).
- [13] S. Brackertz, S. Schlemmer, and O. Asvany, *J. Mol. Spectrosc.* **342**, 73 (2017).
- [14] C. Fábri, M. Quack, and A. G. Császár, *J. Chem. Phys.* **147**, 134101 (2017).
- [15] C. Fábri and A. G. Császár, *Phys. Chem. Chem. Phys.* **20**, 16913 (2018).
- [16] A. G. Császár, C. Fábri, and J. Sarka, *WIREs Comput. Mol. Sci.* **10**, e1432 (2020).
- [17] G. A. Natanson, G. S. Ezra, G. Delgado-Barrio, and R. S. Berry, *J. Chem. Phys.* **81**, 3400 (1984).
- [18] G. A. Natanson, G. S. Ezra, G. Delgado-Barrio, and R. S. Berry, *J. Chem. Phys.* **84**, 2035 (1986).
- [19] D. M. Leitner, G. A. Natanson, R. Berry, P. Villarreal, and G. Delgado-Barrio, *Comput. Phys. Commun.* **51**, 207 (1988).
- [20] J. E. Hunter, D. M. Leitner, G. A. Natanson, and R. Berry, *Chem. Phys. Lett.* **144**, 145 (1988).
- [21] M. P. Deskevich and D. J. Nesbitt, *J. Chem. Phys.* **123**, 084304 (2005).
- [22] M. P. Deskevich, A. B. McCoy, J. M. Hutson, and D. J. Nesbitt, *J. Chem. Phys.* **128**, 094306 (2008).
- [23] F. Uhl, L. Walewski, H. Forbert, and D. Marx, *J. Chem. Phys.* **141**, 104110 (2014).
- [24] H. Schmiedt, P. Jensen, and S. Schlemmer, *Phys. Rev. Lett.* **117**, 223002 (2016).
- [25] H. Schmiedt, P. Jensen, and S. Schlemmer, *Chem. Phys. Lett.* **672**, 34 (2017).
- [26] H. Schmiedt, P. Jensen, and S. Schlemmer, *J. Mol. Spectrosc.* **342**, 132 (2017).
- [27] J. I. Rawlinson, *J. Chem. Phys.* **151**, 164303 (2019).
- [28] L. Pauling, *J. Chem. Phys.* **4**, 673 (1936).
- [29] J. I. Rawlinson, *Nucl. Phys. A* **975**, 122 (2018).
- [30] J. I. Rawlinson, *Rovibrational Dynamics of Nuclei and Molecules*, Ph.D. thesis, University of Cambridge (2020).
- [31] G. Berkolaiko and P. Kuchment, “Introduction to quantum graphs,” in *Mathematical Surveys and Monographs*, Vol. 186 (American Mathematical Society, 2013).
- [32] P. R. Bunker and P. Jensen, *Molecular symmetry and spectroscopy* (NRC Research Press, Ottawa, 2006).
- [33] P. R. Schreiner, S.-J. Kim, H. F. Schaefer III, and P. von Ragué Schleyer, *J. Chem. Phys.* **99**, 3716 (1993).
- [34] N. Biggs, *Algebraic Graph Theory* (Cambridge University Press, 1993).
- [35] P. Árendás, T. Furtenbacher, and A. G. Császár, *J. Math. Chem.* **54**, 806 (2016).